HEAT TRANSFER DURING THE BOILING OF WATER AND FREON-113 AT AN ISOTHERMAL SURFACE

I. N. Dul'kin, N. I. Rakushina,
L. I. Roizen, and V. G. Fastovskii

UDC 536.423.1:536.24

An analytical and experimental study has been made of the heat flow modes (of the $q = f(\vartheta_{B1})$ relation) during the boiling of water and Freon-113 at the isothermal surface of a cylindrical stud. The heat flux was supplied through an end surface of the stud and was dissipated off its lateral surface, at which various modes of pool boiling occurred simultaneously. Test data are compared here with analytical calculations.

The problem of effectively dissipating high heat flux densities is very important in ensuring a reliable operation and in reducing the size of many engineering devices (high-power oscillator tubes, electron guns, fuel elements in nuclear reactors, etc). The use of finned surfaces at which a liquid is made to boil has facilitated the design of compact systems capable of dissipating heat flux densities (per unit base area) many times higher than the first critical heat flux density associated with the boiling of a liquid at an isothermal surface [1]. Such high heat dissipating capabilities are attained by developing the heat exchanger surface ($uh/f > 1$) and by a stable coexistence of various boiling modes at the fin.

For the design of finned heat-exchanger sections it is necessary to establish the relation between the heat flux flowing through a fin, the maximum temperature (at the fin base), the geometry of a fin, its thermal conductivity, and the coefficient of heat transfer to the boiling liquid.

The complexity of an analytical solution to this problem arises because the heat-transfer coefficient varies along the fin surface as a function of the local temperature difference between the fin boiling liquid.

The following analytical calculation of the heat flow modes during the boiling of a liquid at a fin surface applies to a fin of a constant cross section and the experimental results presented here refer to the heat transfer during the boiling of water and Freon-113 at cylindrical copper studs.

Analytical Calculations

The dependence of the local heat-transfer coefficient on the temperature excess is assumed here, as in [2-7], to be a power relation $\alpha = a\vartheta^n$. The factor a and the exponent n remain constant within zones along the fin where the same boiling mode prevails, while the function $\alpha = f(\vartheta)$ approximates the boiling curve for a liquid at an isothermal surface. The values of a and n for various boiling modes of water and Freon-113 are given in Table 1. For the free convection zone we use the generalized data of [8] (water, Freon-113, and methyl alcohol), for the nucleate boiling mode we use the test data and the generalized equations of [9, 10, 11]. For the zone of the transitional boiling mode we use the test data of [2] for Freon-113 and the test data of [12] for water. The heat-transfer coefficient is assumed constant in the zone of film boiling [13, 14]. The boundaries between zones where different boiling modes occur are defined by the incipient temperature of nucleate boiling ϑ_{ib} (between the free convection and the nucleate boiling zone), by the first critical temperature ϑ_{cr_1} (between the nucleate boiling and the transitional boiling zone), and by the second critical temperature ϑ_{cr_2} (between the transitional and the film boiling zone). With the power-law approximation of the boiling curve, these temperatures are determined by the intersection of the $\alpha = f(\vartheta)$ curves for adjacent modes. The values of ϑ_{ib}, ϑ_{cr_1}, and ϑ_{cr_2} used in the calculation are also shown in Table 1.

V. I. Lenin All-Union Electrical-Engineering Institute, Moscow. Translated from Inzhenerno-Fizicheskii Zhurnal, Vol. 19, No. 4, pp. 637-645, October, 1970. Original article submitted October 20, 1969.

TABLE 1. Local Heat Transfer Coefficient as a Function of the Temperature Excess

Zone		Water a	Water n	Freon-113 a	Freon-113 n
Free convection	$0 < \vartheta \leqslant \vartheta_{ib}$	$1{,}16 \cdot 10^{-1}$	1/3	$2{,}16 \cdot 10^{-2}$	1/3
Nucleate boiling	$\vartheta_{ib} < \vartheta \leqslant \vartheta_{cr1}$	$8{,}00 \cdot 10^{-3}$	2	$1{,}10 \cdot 10^{-3}$	2
Transitional boiling	$\vartheta_{cr1} < \vartheta \leqslant \vartheta_{cr2}$	$1{,}41 \cdot 10^{4}$	−2,4	$4{,}40 \cdot 10^{5}$	−4
Film boiling	$\vartheta > \vartheta_{cr2}$	$2{,}51 \cdot 10^{-2}$	0	$1{,}59 \cdot 10^{-2}$	0
Temperature excess, °C	ϑ_{ib}	5		6	
	ϑ_{cr1}	25,9		27,1	
	ϑ_{cr2}	250		72,5	

Assuming that the temperature field in a fin is uniform, that there are no internal heat sources present, and that the thermal conductivity of the fin material is constant, we can write the differential equation of heat conduction through a fin is as follows:

$$f\lambda \frac{d^2\vartheta}{dx^2} = \alpha(\vartheta) u\vartheta. \tag{1}$$

If the power-law relation $\alpha = a\vartheta^n$ is inserted into (1) and this equation is then reduced to the dimensionless form by introducing the variables $X = x/h$, $\Theta = \vartheta/\vartheta_{B1}$, and $\bar{\alpha} = A\Theta^n$ ($A = a\vartheta^n_{B1}/a_f$), we will obtain

$$\frac{d^2\Theta}{dX^2} = K^2 A \Theta^{n+1}, \tag{1a}$$

Equation (1a) is then solved for the following boundary conditions:

for $X = 0$

$$\Theta = 1, \tag{2}$$

for $X = 1$

$$\frac{d\Theta}{dX} = -\frac{\alpha_L h}{\lambda} \Theta^{n_L + 1}, \tag{3}$$

for $X = X_{Ej}$

$$\Theta_{Ej} = \Theta_{B(j+1)}, \tag{4}$$

$$\left(\frac{d\Theta}{dX}\right)_{Ej} = \left(\frac{d\Theta}{dX}\right)_{B(j+1)}. \tag{5}$$

From (3) and (5) we derive an expression for the temperature gradient across any zone j:

$$\frac{d\Theta}{dX} = -K\left[\frac{2A}{n+2}\left(\Theta^{n+2} - \Theta_E^{n+2}\mu\right)\right]_j^{1/2}. \tag{6}$$

When j = L, it follows from (6) and the boundary condition (3) that

$$\mu_L = 1 - \mathrm{Bi}\,\frac{(n_L + 2)(a\vartheta^n)_L}{2a_f}. \tag{7}$$

If the heat transfer at the tip is negligible, then $\mu_L = 1$. When $j < L$, then μ_j is determined from the boundary condition (5) by the recurrence formula

$$\mu_j = 1 - \frac{(n_j + 2)(a\vartheta_B^n)_{j+1}}{(n_{j+1} + 2)(a\vartheta_E^n)_j}\left[1 - (T_*^{n+2}\mu)_{j+1}\right]. \tag{8}$$

Equation (8) is valid in the general case (function $\alpha = f(\vartheta)$ may have first-order discontinuities at the zone boundaries). If the function is continuous, then $(a\vartheta^n_B)_{j+1}/(a\vartheta^n_E)_j = 1$. Integrating (6) and introducing $T = \vartheta_E/\vartheta$ yields, after a few transformations,

$$I(T, \mu) \equiv \sqrt{\frac{n+2}{2}}\, T^{-\frac{n}{2}} \int_T^1 \frac{dy}{y^{\left(1-\frac{n}{2}\right)}\sqrt{1 - y^{n+2}\mu}} = K\sqrt{\frac{a\vartheta^n}{a_f}}\,(X_E - X). \tag{9}$$

The values of the integrals $I(T, \mu)$ are given here for $n = 0$ (film boiling mode), $n = 1/3$ (free conversion region), $n = 2$ (nucleate boiling mode), $n = -1$, -2.4, and -4 (various power-law relations for $\alpha = f(\vartheta)$ in the region of the transitional boiling mode):

for $n = 0$

$$I(T, \mu) = \ln \frac{1+\sqrt{1-T^2\mu}}{T(1+\sqrt{1-\mu})}; \tag{10}$$

for $n = 1/3$

$$I(T, \mu) \cong 0.463 T^{-\frac{1}{6}} \mu^{-\frac{1}{14}} \ln \frac{1+\sqrt{1-\tilde{y}}}{1-\sqrt{1-\tilde{y}}} \Bigg|_{\tilde{y}=\mu}^{\tilde{y}=\mu T^{\frac{7}{3}}}; \tag{11}$$

for $n = 2$

$$I(T, \mu) = \begin{cases} \dfrac{F(\varphi_1, \alpha) - F(\varphi_2, \alpha)}{T\mu^{1/4}} & \text{when } \mu > 0, \quad (12a) \\ \text{where } \varphi_1 = \arccos(T\mu^{1/4}); \quad \varphi_2 = \arccos(\mu^{1/4}); \quad \alpha = & (12b) \\ \quad = \arcsin \dfrac{\sqrt{2}}{2} = 45^\circ, & (12c) \\ \sqrt{2}(1-T)T^{-1} & \text{when } \mu = 0, \\ \dfrac{\sqrt{2}(2-\sqrt{2})}{T|\mu|^{1/4}} [F(\varphi_2, \alpha) - F(\varphi_1, \alpha)] & \text{when } \mu < 0, \\ \text{where } \varphi_1 = \operatorname{arctg}\left[(1+\sqrt{2}) \dfrac{1+T|\mu|^{1/4}}{1-T|\mu|^{1/4}}\right]; \\ \varphi_2 = \operatorname{arctg}\left[(1+\sqrt{2}) \dfrac{1+|\mu|^{1/4}}{1-|\mu|^{1/4}}\right]; \\ \alpha = \arcsin\left[\left(\dfrac{4\sqrt{2}}{3+2\sqrt{2}}\right)^{1/2}\right] \cong 80^\circ; \\ F(\varphi, \alpha) \text{ — an elliptical integral of the first kind;} \end{cases}$$

for $n = -1$

$$I(T, \mu) = \sqrt{2}\,[\sqrt{1-\mu T} - \sqrt{T(1-\mu)}]; \tag{13}$$

for $n = -2.4$

$$I(T, \mu) = 2.235 T^{6/5} \mu^{-3} \left(\frac{1}{5}\tilde{y}^5 + \frac{2}{3}\tilde{y}^3 + \tilde{y}\right) \Bigg|_{\tilde{y}=\sqrt{\mu-1}}^{\tilde{y}=\sqrt{\mu T^{-2/5}-1}}; \tag{14}$$

for $n = -4$

$$I(T, \mu) = T^2\mu^{-1})\sqrt{\mu T^{-2}-1} - \sqrt{\mu-1}). \tag{15}$$

With the aid of (9) and the boundary conditions (4) one determines the equation relating the referred characteristic parameter K to the temperature ϑ_{B1} at the base and ϑ_{EL} at the tip:

$$K = \sum_{i=1}^{L} \sqrt{\frac{a_f}{(a\vartheta_B^n)_i}}\, I_i(T_*, \mu). \tag{16}$$

It follows from (9) and (16) that the length of zone j can be calculated by the formula

$$(X_E - X_B)_j = \frac{\left[\dfrac{a_f}{(a\vartheta_B^n)_j}\right]^{1/2} I_j(T_*, \mu)}{K}. \tag{17}$$

After having defined the coordinates of the beginning (B) and the end (E) of each zone according to Eq. (17), the temperature profile in zone j can be conveniently calculated by the formula

$$\left(\frac{T}{T_*}\right)_j^{n_j/2} \frac{I_j(T,\mu)}{I_j(T_*,\mu)} = \left(\frac{X_E - X}{X_E - X_B}\right)_j .$$

From Eq. (6) for j = 1 and X = 0 one can then determine the heat flux density transmitted through a fin:

$$q = \left\{\frac{2\alpha_f}{\mathrm{Bi}}\left[\left(\frac{a\vartheta_B^{n+2}}{n+2}\right)(1-T_*^{n+2}\mu)\right]_1\right\}^{1/2},$$

where μ_1 is defined by Eqs. (7) and (8). If the heat flow from the tip is negligible ($\mu_L = 1$), then Eq. (19) becomes

$$q = \left\{\frac{2\alpha_f}{\mathrm{Bi}}\sum_{i=1}^{L}\left[\left(\frac{a\vartheta_B^{n+2}}{n+2}\right)(1-T_*^{n+2})\right]_i\right\}^{1/2}.$$

Experimental Study

In order to verify the calculated relations, the heat dissipation off cylindrical studs 1.4 cm in diameter and 6.6, 4.4, 2.65, and 1.25 cm long was studied with water and Freon-113, pool-boiling under atmospheric pressure. The test apparatus is shown schematically in Fig. 1b. A cylindrical copper stud was made integrally with the large core of a 3-Kw electric heater. The stud was immersed in a 10-liter boiler vessel through a thin (0.3 mm) wall of stainless steel. The liquid in the vessel was maintained at the saturation temperature by means of two 1-kW electric boilers. Visual observations were made and photographs were taken through sight windows. The boiler vessel with the test stud and the heater were mounted on a movable frame so that the stud position could be varied. Tests were performed with the stud in the horizontal and in the vertical position (in the latter case with the tip up and down). For the purpose of measuring the temperature profile, 1-mm diameter holes were drilled into the stud along its surface and Chromel–Alumel thermocouples made of 0.2-mm wire and covered with a 50 μm thick ceramic insulation were sealed into them. Four thermocouples were placed along the thermally insulated stud section, the remaining thermocouples were placed along the section immersed in liquid. The temperature at the stud base was determined by the point where the temperature profile intersected the base coordinate, while the heat flux

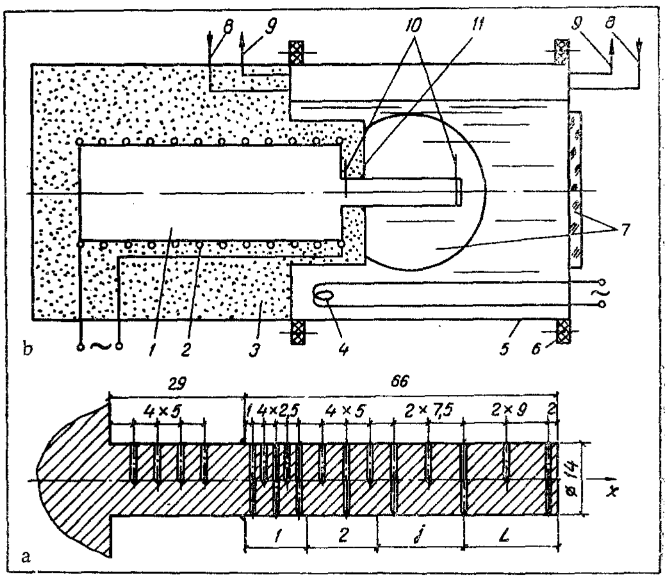

Fig. 1. Schematic diagram of the test stud (a) and the experimental apparatus (b): 1) heater core with the test stud; 2) electric heater; 3) insulation; 4) electric boiler; 5) boiler vessel housing; 6) sealing; 7) sight window; 8) condensate recuperator; 9) vapor outlet; 10) thermocouples; 11) stainless steel wall (0.3 mm thick).

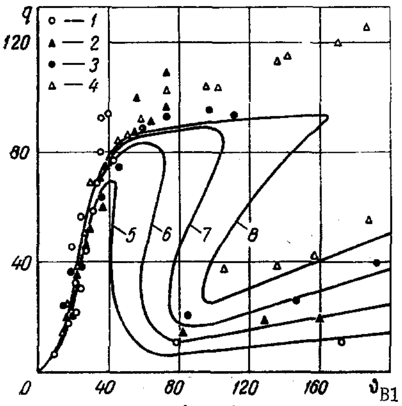

Fig. 2

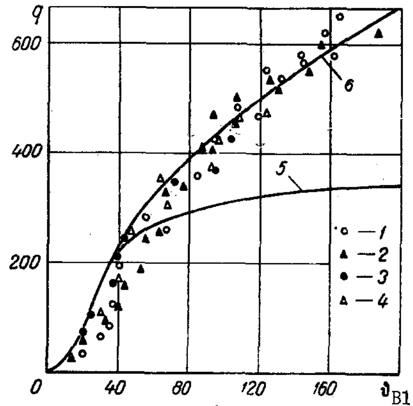

Fig. 3

Fig. 2. Heat-flux density q, W/cm^2), as a function of the temperature excess ϑ_{B1}, °C, at the base during the boiling of Freon-113 at horizontal copper studs, D = 1.4 cm: 1-4) test data; 5-8) calculated curves for stud lengths 1.25 cm (K = 0.14), 2.65 cm (K = 0.3), 4.4 cm (K = 0.5), and 6.6 cm (K = 0.75) respectively.

Fig. 3. Heat flux density q, W/cm^2, as a function of the temperature excess ϑ_{B1}, °C, at the base during the boiling of water at vertical copper studs, D = 1.4 cm: 1-4) test data for stud lengths 1.25 cm (K = 0.1785), 2.65 cm (K = 0.379), 4.4 cm (K = 0.628), and 6.6 cm (K = 0.945), respectively; 5, 6) calculated curves for compound boiling at all tested studs, with n = –2.4 and n = –1 in the zone of transitional boiling respectively.

was determined by the temperature gradient across the thermally insulated section. The thermocouple indications were read on a P-307 potentiometer. The temperature profile was also continuously recorded with an automatically operating ÉPP-09-3M potentiometer, which recorded the temperatures of transition from compound boiling (coexistence of several different boiling modes) to film boiling along the entire stud and also the temperatures of the reverse transition. Simultaneously with the recording of the temperature profile, the respective boiling modes were photographed with illumination from flash bulbs. All tests were performed under steady-state conditions.

In order to account for heat leakage, taring tests were performed at the location where the stud had been let into the boiler vessel. The stud was cut off flush with the wall, with a Teflon tube 1.4 cm in diameter and 0.1 cm thick clamped on the stud tip and then filled with asbestos powder. In this way, insulation was provided between the stud tip and the liquid while the wall remained under the same conditions as in the basic tests. The heat loss curves thus obtained were then used in the evaluation of test data.

In Fig. 2 are shown the test data for boiling Freon-113 at horizontal studs, and also the $q = f(\vartheta_{B1})$ curves for the same studs calculated by Eq. (19). The calculated curves agree closely with the test data (the tested values of q exceed the calculated values by not more than 30% within the range of high ϑ_{B1} values for each stud).

The calculated temperatures of transition from compound boiling to film boiling along the entire stud (corresponding in Fig. 2 to the maximum values of q for each stud) as well as the calculated temperatures of the reverse transition (corresponding here to the minimum values of q on the lower branches of the curves) are also respectively in close agreement with the tested temperatures. This correlation between theoretical $\alpha = f(\vartheta)$ data (calculated from the boiling curves for a horizontal surface) with the experimental data indicates that, apparently, there is a rather weak interplay between the zones of different boiling modes for Freon-113. Visual observations have confirmed this.

In Fig. 3 are shown the test data and the calculated curves for the compound boiling of water at the studs. The character of water boiling differs substantially from that of Freon-113 boiling. A strong interplay between the zones of nucleate and of transitional boiling was observed. At $\vartheta_{B1} > 30$–40°C, vapor from both zones merged into one bubble the dimensions and separation frequency of which increased with higher

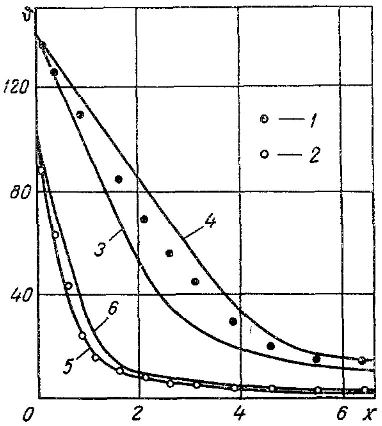

Fig. 4. Temperature profile along a horizontal copper stud (D = 1.4 cm, h = 6.6 cm) during the boiling of Freon-113 and water. Freon-113: 1) test data; 3, 4) calculated according to (18) with $n = -1$ and $n = -4$ in the zone of transitional boiling; water: 2) test data; 5, 6) calculated according to (18) with $n = -1$ and $n = -2.4$ in the zone of transitional boiling.

ϑ_{B1} values. A bubble separated from the fin surface off a narrow strip next to the base (0.3-0.4 cm wide when $\vartheta_{B1} \cong 40$°C and up to 1-1.2 cm wide when $\vartheta_{B1} \cong 200$°C). Practically no boiling took place along the remaining part of the stud. Curve 5 (Fig. 3), which has been plotted according to Eq. (20) with the aid of the boiling curve for an isothermal surface in all zones (Table 1), lies much lower than the curves based on test data. Calculations made according to the same equation but with $n = -1$ and $a = q_{cr1} = 125$ W/cm^2, i.e., for a constant local heat flux density in the transitional boiling zone (curve 6) agree closely with the test data. This is confirmed in Fig. 4 showing tested and calculated temperature profiles along the 6.6-cm stud. One can see that temperature variations corresponding to transitional and fully developed nucleate boiling of water occur over a distance comparable with the separation dimension of a bubble (~ 1.2 cm). Due to an interplay between the two zones at a high temperature gradient across the stud, apparently, the rate of heat transfer in the region of transitional boiling does not increase according to the boiling curve but much less sharply. This conclusion agrees with the data in [1], where the boiling of water was studied at finned anodes of high-power oscillator tubes (vapotrons).

In Fig. 4 are shown also the corresponding experimental (1) and calculated (3, 4) temperature profiles during the boiling of Freon-113.

The tests have not revealed any significant effect of the stud position on the $q = f(\vartheta_{B1})$ relation. When the different boiling modes coexist, the maximum difference between heat flux values at various stud positions has not been found to exceed 5%. During film boiling, on the other hand, the heat flux along an entire stud is approximately 20% higher in a vertical position than in a horizontal position.

NOTATION

ϑ	is the temperature excess (difference between the fin temperature and the boiling point of a liquid), °C;
$\Theta = \vartheta/\vartheta_{B1}$, $T = (\vartheta/\vartheta_B)_j$, $T_* = (\vartheta_E/\vartheta_B)_j$	are the dimensionless temperature excesses;
x	is the coordinate, cm;
h	is the fin length, cm;
$X = x/h$	is the dimensionless coordinate;
D	is the diameter of cylindrical stud, cm;
u	is the circumference of a transverse stud cross section, cm;
f	is the area of a transverse stud cross section, cm^2;
q	is the heat flux density transmitted through the fin (per unit transverse cross-section area), W/cm^2;
λ	is the thermal conductivity of the stud material;
α	is the local heat-transfer coefficient, W/cm^2·°C;
$\bar{\alpha} = \alpha/a_f$	is the dimensionless local heat-transfer coefficient;
a	is the factor W/cm^2(°C)$^{n+1}$;
n	is the exponent;
$A = a\vartheta_{B1}^n/a_f$, μ	are the dimensionless coefficients;
$K = h(a_f u/\lambda f)^{1/2}$	is the referred characteristic fin parameter;
$Bi = a_f f/\lambda u$	is the referred Biot number;
$I(T, \mu)$	is the integral defined in Eq. (9);
y, $\tilde{y}$	are the integration variables.

Subscripts

1, 2, ..., j, j + 1, ..., L	are the consecutive numbers of heat transfer zones from the base to the tip of a fin;
Bj	is at the beginning of a zone (at the left-hand boundary of zone j);
Ej	is at the end of a zone (at the right-hand side of zone j, Fig. 1);
ib	is the beginning of nucleate boiling;
cr1	is the first critical;
cr2	is the second critical;
f	is the film boiling.

LITERATURE CITED

1. Sh. A. Bertere, Heat and Mass Transfer [in Russian], Vol. 9, Minsk (1968).
2. K. W. Haley and J. W. Westwater, Proceedings of the Third International Heat-Transfer Conference, Vol. 3, Chicago (1966).
3. F. S. Lai and Y. Y. Hsu, AIChE J., 13, No. 4 (1967).
4. T. Tsuchiya, M. Ouchi, and T. Takeyama, Trans. Japan. SME, 33, 253 (1967).
5. L. I. Roizen and I. N. Dul'kin, Izv. VUZ. Énergetika, No. 3 (1968).
6. S. A. Kovalev and L. F. Smirnova, Teplofiz. Vys. Temp. No. 4 (1968).
7. S. A. Kovalev, Teplofiz. Vys. Temp., No. 5 (1964).
8. Lippert and Dougal, Teploperedacha, No. 3 (1968).
9. S. S. Kutateladze, Heat Transfer during Condensation and Boiling [in Russian], Mashgiz, Moscow (1952).
10. V. M. Borishanskii, Kholodil'naya Tekh., No. 7 (1967).
11. V. M. Rohsenow, Trans. ASME, 74, 969-976 (1952).
12. S. Ishigai and T. Kuno, Bull. Japan. SME, 9, No. 34 (1966).
13. V. M. Borishanskii and B. S. Fokin, Inzh. Fiz. Zh., 8, No. 3 (1965).
14. B. P. Breen and J. W. Westwater, Chem. Eng. Progress, 58, No. 7 (1962).